Title	A coupled 'AB' system: Rogue waves and modulation instabilities
Author(s)	Wu, C; Grimshaw, RHJ; Chow, KW; CHAN, HN
Citation	Chaos, 2015, v. 25, p. 103113:1-9
Issued Date	2015
URL	http://hdl.handle.net/10722/226326
Rights	Chaos. Copyright © American Institute of Physics.; Copyright (2015) American Institute of Physics. This article may be downloaded for personal use only. Any other use requires prior permission of the author and the American Institute of Physics. The following article appeared in (Chaos, 2015, v. 25, p. 103113:1-9) and may be found at (http://dx.doi.org/10.1063/1.4931708).; This work is licensed under a Creative Commons Attribution-NonCommercial-NoDerivatives 4.0 International License.

A coupled "*AB*" system: Rogue waves and modulation instabilities

C. F. Wu,[1] R. H. J. Grimshaw,[2] K. W. Chow,[3,a)] and H. N. Chan[3]
[1]*Department of Mathematics, University of Hong Kong, Pokfulam, Hong Kong*
[2]*Department of Mathematics, University College London, London WC1E 6BT, United Kingdom*
[3]*Department of Mechanical Engineering, University of Hong Kong, Pokfulam, Hong Kong*

(Received 13 May 2015; accepted 14 September 2015; published online 25 September 2015)

Rogue waves are unexpectedly large and localized displacements from an equilibrium position or an otherwise calm background. For the nonlinear Schrödinger (NLS) model widely used in fluid mechanics and optics, these waves can occur only when dispersion and nonlinearity are of the same sign, a regime of modulation instability. For coupled NLS equations, rogue waves will arise even if dispersion and nonlinearity are of opposite signs in each component as new regimes of modulation instability will appear in the coupled system. The same phenomenon will be demonstrated here for a coupled "*AB*" system, a wave-current interaction model describing baroclinic instability processes in geophysical flows. Indeed, the onset of modulation instability correlates precisely with the existence criterion for rogue waves for this system. Transitions from "elevation" rogue waves to "depression" rogue waves are elucidated analytically. The dispersion relation as a polynomial of the fourth order may possess double pairs of complex roots, leading to multiple configurations of rogue waves for a given set of input parameters. For special parameter regimes, the dispersion relation reduces to a cubic polynomial, allowing the existence criterion for rogue waves to be computed explicitly. Numerical tests correlating modulation instability and evolution of rogue waves were conducted.
[http://dx.doi.org/10.1063/1.4931708]

In the oceans, abnormally large waves from a calm background or relatively tranquil wave train can occur and have been termed "rogue waves". These waves obviously pose immense danger to shipping and offshore structures, and have been known to sailors for nearly a century. Systematic scientific studies in fluid mechanics started only about twenty years ago. In the past few years, similar investigations have been pursued intensively in many disciplines as "extreme and rare events in physics", after such surprisingly large waves were observed in an optical fiber. The nonlinear Schrödinger (NLS) equation is a widely used model where the rogue waves are expressed as an algebraic expression in space and time. The goal of this work is to extend such considerations to a coupled "wave envelope-mean flow" system relevant in geophysical flows. Similar to coupled NLS equations, the remarkable feature here is that multiple wave packets can induce additional regimes of modulation instability. Nonlinear couplings thus permit new domains of existence of rogue waves, which are otherwise prohibited if each waveguide is operating alone by itself.

I. INTRODUCTION

Rogue waves are unexpectedly large displacements from an equilibrium position or an otherwise tranquil background, constituting a class of nonlinear waves[1] localized in both space and time. Sailors have been aware of such dangerous waves for a long time. More than 20 large vessels were lost at sea in the period 1969–1994 presumably due to these large amplitude waves, resulting in significant casualties.[2] Systematic scientific studies in fluid mechanics only started about 20 years ago, employing both deterministic and probabilistic approaches.[3–6] Many factors have been proposed, e.g., soliton interactions, wave-current dynamics, geometric focusing, and modulation instabilities. Rogue internal waves utilizing long wave models have also been considered.[7] An important milestone occurred when such abnormal waves were measured experimentally using an optical fiber as an waveguide.[8] Since then there has been an explosion of research activities looking into rogue waves in various physical settings, e.g., liquid helium, microwave cavities, and plasmas.[6]

In many physical applications, e.g., fluid dynamics and optics, the evolution of a slowly varying wave packet is typically governed by the NLS equation.[9,10] For two or more packets with the same group velocity, the corresponding model is a system of coupled NLS equations.[11,12] The NLS model with one single component is

$$i\Psi_t + \Psi_{xx} + \delta\Psi^2\Psi^* = 0, \quad \delta = \text{a real parameter}, \tag{1}$$

where the slowly varying envelope Ψ is expressed in the reference frame moving with a group velocity frame (x). The Peregrine breather

$$\Psi = m\exp(i\delta m^2 t)\left\{1 - \frac{2(1+2i\delta m^2 t)}{\delta m^2\left(x^2 + 2\delta m^2 t^2 + \frac{1}{2\delta m^2}\right)}\right\}, \; m \text{ real}, \tag{2}$$

a)Author to whom correspondence should be addressed. Electronic mail: kwchow@hku.hk. Fax: (852) 2858 5415.

localized algebraically both in x and t, is frequently used as a model of a rogue wave.[13] This rogue wave can be regarded as a long wave (infinite wavelength) limit of a breather (a pulsating mode).[14] The Kuznetsov-Ma breather is periodic in the direction of the propagation variable (t here), while the Akhmediev breather is periodic in the transverse variable (x here). Each will tend to the Peregrine breather in the limit of an indefinitely large period.

The Peregrine breather has a maximum amplitude of three times the background, and occurs only in the regime where nonlinearity and dispersion are of the same sign ($\delta > 0$). This regime also defines the domain of modulation instability, where a small disturbance on a plane (or continuous) wave can grow exponentially as a result of the interplay between nonlinearity and dispersion. This intimate connection between existence of rogue waves and onset of modulation instabilities has been recognized by researchers, using NLS,[15] derivative NLS,[16] and Korteweg-de Vries[17] equations as models. For coupled NLS equations, from the perspective of applications in fluid dynamics, the roles and relevance of non-symmetric wave pattern[10] and oblique wave packets propagation can be considered, especially from the perspective of rogue wave formation.[11,12] From the viewpoint of nonlinear science, coupled equations tend to bring additional degrees of freedom and intriguing dynamical behavior.[18] For coupled NLS equations, new modulation instabilities can indeed occur even if dispersion and nonlinearity are of opposite signs in each component, leading to the existence of rogue waves.[19] The main goal of this work is to consider a similar coupled system arising from evolution of wave packets in geophysical fluid dynamics.

The remarkable feature of all these studies is that elegant theoretical techniques allow analytical solutions to be found with potential physical significance, and these localized waves may be verified in a laboratory setting. Indeed, the Peregrine breather could be observed in a wave tank.[20] However, higher order nonlinear effects, modeled by the Dysthe equation, will destroy the recurrence character of the breather through the asymmetric broadening of the spectrum.[20] Higher order ("super") rogue waves with amplitude five times the background have also been detected in an experiment.[21]

The structure of the present paper is as follows. First, the formulation of the *AB* system as documented in the literature will be presented in Section II. This system is made up of one single slowly varying envelope and a wave-induced mean flow arising in a geophysical fluid dynamics setting as a model for baroclinic instability. In this paper, our contribution is to investigate an extension of this model where the system contains *two* short wave envelopes. The presence of multiple short wave envelopes leads to new regimes of modulation instability, and hence new domains of existence of rogue waves, similar to the situation for coupled NLS equations.[19] Novel features of rogue waves regarding transitions between "elevation" modes and "depression" modes are elucidated in Section III. Further features of nonlinear dynamics, e.g., multiple eigenvalues and special parameter regimes, are presented in Section IV. Remarkably, we show in Section V that the criterion for the existence of rogue waves for this system matches precisely with the condition of onset of modulation instability. We conclude in Section VI.

II. FORMULATION

The so-called "*AB*" system as studied earlier in the literature arises as an asymptotic reduction of special classes of two-layer geophysical flows which support baroclinic instability processes through appropriate vertical shear. In this formulation, A is a complex valued envelope and B_0 is the wave-induced modification of the basic flow by the wave packet. The governing system is[22–24]

$$\left(\frac{\partial}{\partial T}+c_1\frac{\partial}{\partial X}\right)\left(\frac{\partial}{\partial T}+c_2\frac{\partial}{\partial X}\right)A = n_1 A - n_2 A B_0,$$
$$\left(\frac{\partial}{\partial T}+c_2\frac{\partial}{\partial X}\right)B_0 = \left(\frac{\partial}{\partial T}+c_1\frac{\partial}{\partial X}\right)|A|^2, \tag{3}$$

where c_1 and c_2 are the respective group velocities; T and X are time and space, respectively, and n_1 and n_2 are real parameters. Extension to continuous shear and stratification profiles is feasible.[23] Next we change to characteristic coordinates and rescale

$$x = X - c_1 T, \quad t = T - \frac{X}{c_2}, \quad n_2 c_2 B_0 = (c_1 - c_2)^2 B, \tag{4}$$

and hence the *AB* system occurring in the recent literature is

$$A_{xt} = \lambda A - AB, \quad B_x = \sigma\left(|A|^2\right)_t,$$
$$\lambda = \frac{n_1 c_2}{(c_1 - c_2)^2}, \quad \sigma = \frac{n_2}{(c_1 - c_2)^2}, \tag{5}$$

where λ, σ are real constants. When A is real valued, a reduction to the integrable sine-Gordon equation can be made. Various solutions can then be found, e.g., periodic patterns have been evaluated in closed form.[24] Breathers (pulsating modes) have been calculated by generalized Darboux transformations.[25] Rogue waves have been derived using similar techniques, in a parameter regime where rogue waves are assumed implicitly to exist.[26]

In our opinion, it will be useful and illuminating to elucidate the existence condition of rogue waves in terms of parameters of the differential equations, and also in terms of the physical mechanisms relating to their existence, e.g., modulation instability.

Along the line of reasoning introduced earlier, our main contribution in this work is to enrich the nonlinear dynamics by considering two propagating wave packets. The resulting coupled evolution equations are

$$(A_1)_{xt} = \lambda A_1 - A_1 B, \tag{6a}$$

$$(A_2)_{xt} = \lambda A_2 - A_2 B, \tag{6b}$$

$$B_x = \sigma(|A_1|^2 + |A_2|^2)_t, \tag{6c}$$

where A_1 and A_2 are the packets of short waves and B is the mean flow. We have assumed that the coefficients of A_1B, A_2B in Eqs. (6a) and (6b) are identical, otherwise the equations might not be integrable. Eqs. (6a)–(6c) constitute the main focus of this work. Instead of the Darboux transformation, the Hirota bilinear method[27,28] will be applied, as the latter has been demonstrated to be useful in the derivation of multi-soliton for integrable systems over the past 40 years.[28] This bilinear method will also be shown here to be effective in the calculation of rogue waves.[29]

It will be instructive to elucidate the contrast with the intensively studied integrable coupled NLS or Manakov equations. In terms of theoretical techniques, both the Darboux transformation[30] and the Hirota bilinear method[31] have been applied for the Manakov case, but only the Darboux technique has been utilized for the *AB* system.[25,26] Our contribution is to apply the Hirota bilinear method to such *AB* system.

In terms of physics, situations where the self phase modulation (SPM) and cross phase modulation (XPM) coefficients are of the same or opposite signs have been studied for the generalized coupled NLS equations,[32] but our present effort focuses on the case where the intensity terms $|A_1|^2$, $|A_2|^2$ are of the same sign. Indeed, there are differences between the coupled NLS system and the coupled *AB* system. Cubic nonlinearity occurs in coupled NLS system, and the system is integrable only if the SPM and XPM coefficients are equal in magnitude (Manakov equations). As cubic terms are absent in Eq. (6), one can always scale the amplitude such that the coefficients of the intensity terms $|A_1|^2$, $|A_2|^2$ are equal in magnitude.

To initiate the bilinear method, we first implement the dependent transformations to rewrite Eq. (6)

$$A_1 = \frac{g}{f}, \quad A_2 = \frac{h}{f}, \quad B = 2(\log f)_{xt}, \quad g, h \text{ complex}, \ f \text{ real}, \tag{7}$$

$$(D_xD_t - \lambda)g\,.f = 0, (D_xD_t - \lambda)h\,.f = 0,$$
$$(D_x{}^2 - C)f\,.f = \sigma(gg^* + hh^*), \quad C = \text{constant},$$

where the bilinear operator is defined by[27,28]

$$D_x^m D_t^n g.f = \left(\frac{\partial}{\partial x} - \frac{\partial}{\partial x'}\right)^m \left(\frac{\partial}{\partial t} - \frac{\partial}{\partial t'}\right)^n g(x,t)f(x',t')|_{x'=x,t'=t}.$$

The appropriate expansion to obtain breathers is

$$g = \rho\, \exp\,[i(\alpha x - \lambda t/\alpha)]\{1 + a_1 \exp\,(px - \Omega t + \eta_1) + a_2 \exp\,(p^* x - \Omega^* t + \eta_2) + Ma_1a_2 \exp[(p+p^*)x - (\Omega + \Omega^*)t + \eta_1 + \eta_2]\}, \tag{8a}$$

$$h = \rho\, \exp[i(\beta x - \lambda t/\beta)]\{1 + b_1 \exp(px - \Omega t + \eta_1) + b_2 \exp(p^* x - \Omega^* t + \eta_2) + Mb_1b_2 \exp[(p+p^*)x - (\Omega + \Omega^*)t + \eta_1 + \eta_2]\}, \tag{8b}$$

$$f = 1 + \exp(px - \Omega t + \eta_1) + \exp(p^* x - \Omega^* t + \eta_2) + M \exp[(p+p^*)x - (\Omega + \Omega^*)t + \eta_1 + \eta_2]\}, \tag{8c}$$

with a_1, a_2, b_1, b_2, p, Ω being complex, α, β, M being real, and η_1, η_2 being arbitrary complex phase factors. From the bilinear equations,

$$a_1 = \frac{i(\alpha\Omega + p\lambda/\alpha) - p\Omega}{i(\alpha\Omega + p\lambda/\alpha) + p\Omega}, \quad a_2 = \frac{1}{a_1^*}, \tag{8d}$$

$$b_1 = \frac{i(\beta\Omega + p\lambda/\beta) - p\Omega}{i(\beta\Omega + p\lambda/\beta) + p\Omega}, \quad b_2 = \frac{1}{b_1^*}, \tag{8e}$$

$$M = \frac{\lambda(p^*\Omega - p\Omega^*)^2 - pp^*\Omega\Omega^*(p - p^*)(\Omega - \Omega^*)}{\lambda(p^*\Omega - p\Omega^*)^2 - pp^*\Omega\Omega^*(p + p^*)(\Omega + \Omega^*)}. \tag{8f}$$

The dispersion relation for Ω in terms of p is

$$\left[\alpha^2\beta^2 + (2\sigma\rho^2 + p^2)(\alpha^2 + \beta^2 + p^2) + 2\sigma\rho^2p^2\right]\Omega^4 + 2(\alpha^2 + \beta^2 + 2p^2 + 4\sigma\rho^2)\lambda p\Omega^3 + \left[(\alpha^2 + \beta^2 + p^2 + 2\sigma\rho^2)\left(\frac{1}{\alpha^2} + \frac{1}{\beta^2}\right) + 2\right]\lambda^2p^2\Omega^2 + 2\left(\frac{1}{\alpha^2} + \frac{1}{\beta^2}\right)\lambda^3p^3\Omega + \frac{\lambda^4p^4}{\alpha^2\beta^2} = 0. \tag{9}$$

From earlier studies,[29] only the long wave regime ($p \to 0$) is significant, and hence we write

$$\Omega = p[\Omega_0 + O(p)] \tag{10}$$

with Ω_0 satisfying

$$\left[\alpha^2\beta^2 + 2\sigma\rho^2(\alpha^2 + \beta^2)\right]\Omega_0^4 + 2(\alpha^2 + \beta^2 + 4\sigma\rho^2)\lambda\Omega_0^3 + \left[(\alpha^2 + \beta^2 + 2\sigma\rho^2)\left(\frac{1}{\alpha^2} + \frac{1}{\beta^2}\right) + 2\right]\lambda^2\Omega_0^2 + 2\left(\frac{1}{\alpha^2} + \frac{1}{\beta^2}\right)\lambda^3\Omega_0 + \frac{\lambda^4}{\alpha^2\beta^2} = 0. \tag{11}$$

With the choice $\exp(\eta_1) = \exp(\eta_2) = -1$ and a Taylor expansion of Eq. (6) for small p, we obtain rogue waves for the coupled *AB* system as

$$A_1 = \rho\, \exp\left(i\alpha x - \frac{i\lambda t}{\alpha}\right)\frac{g_2}{f_2},$$
$$A_2 = \rho\, \exp\left(i\beta x - \frac{i\lambda t}{\beta}\right)\frac{h_2}{f_2},$$
$$B = 2\,(\log f_2)_{xt}, \tag{12}$$

where

$$
\begin{aligned}
f_2 &= M_2 + (x - at)^2 + b^2 t^2, \\
g_2 &= \frac{4[i(a^2\alpha^3 + b^2\alpha^3 + a\alpha\lambda)x - i\alpha(a^2 + b^2)(a\alpha^2 + \lambda)t - \alpha^2(a^2 + b^2)]}{(a\alpha^2 + \lambda)^2 + b^2\alpha^4} + f_2, \\
h_2 &= \frac{4[i(a^2\beta^3 + b^2\beta^3 + a\beta\lambda)x - i\beta(a^2 + b^2)(a\beta^2 + \lambda)t - \beta^2(a^2 + b^2)]}{(a\beta^2 + \lambda)^2 + b^2\beta^4} + f_2, \\
M_2 &= -\frac{a(a^2 + b^2)}{b^2\lambda}, \\
\Omega_0 &= a + ib.
\end{aligned} \tag{13}
$$

The real and imaginary parts of the complex frequency Ω_0 (a and b, respectively) must be determined (usually numerically) from the dispersion relation Eq. (11) (a fourth order polynomial), after the properties of the system (σ, λ of Eq. (6)) and the input wavenumbers (α, β) are given. Special cases outlined in Section IV will permit a reduction to a cubic equation. As usual, a rogue wave here is algebraically localized in both x and t, similar to the NLS equation and other intensively studied models.

TABLE I. Complex angular frequencies Ω_0 for typical values of input wave numbers and *positive* values of σ.

α	β	λ	σ	Ω_0	M_2
2	1	2	1	$-0.946 \pm 0.845i$	1.0667
2	1	2	2	$-0.841 \pm 0.744i$	0.958
4	2	4	1	$-0.699 \pm 0.440i$	0.615
4	2	4	2	$-0.574 \pm 0.454i$	0.373

TABLE II. Complex angular frequencies Ω_0 for typical values of input wave numbers and *negative* values of σ.

α	β	λ	σ	Ω_0	M_2
2	1	2	-1	$-0.840 \pm 0.410i$	2.186
2	1	2	-2	$-0.816 \pm 0.488i$	1.548
4	2	4	-1	No complex roots	
4	2	4	-2	$-0.440 \pm 0.145i$	1.115

III. WAVE PROFILES

For genuinely complex Ω_0, f is generally nonzero (and hence nonsingular rogue wave exists) if M_2 is positive. There exists an invariant of motion

$$\int [\sigma(A_1 A_1^* + A_2 A_2^*)^2/2 - (A_1)_x (A_1^*)_x - (A_2)_x (A_2^*)_x] dx$$

as the time derivative of this quantity vanishes (integral being taken over the entire spatial domain with vanishing boundary conditions in the far field). Consequently, similar to the scenario for the intensively studied coupled nonlinear Schrödinger (Manakov) equations, "elevations" above the mean level must be accompanied by "depressions" to conserve the integral for $\sigma < 0$. For $\sigma > 0$, this feature remains broadly true for all the numerical cases we have tested. In terms of wave profiles, the *AB* system exhibits some similarities with the Manakov equations. The rogue wave of the single component *AB* system

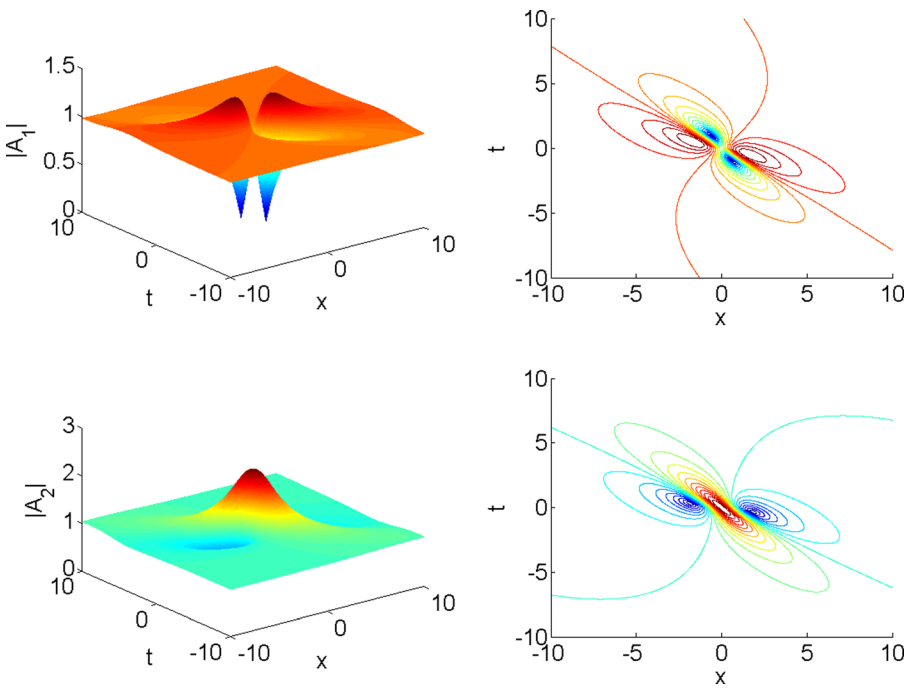

FIG. 1. Rogue waves ($|A_1|$ in the top panel, $|A_2|$ in the bottom panel) and the corresponding contour plots as given in Eqs. (12) and (13) with $\alpha = 2$, $\beta = 1$, $\lambda = 2$, $\sigma = 1$, $\rho = 1$, and $\Omega_0 = -0.946 \pm 0.845i$. $|A_1|$ displays a four-petal configuration, while $|A_2|$ will be termed an elevation rogue wave in this context.

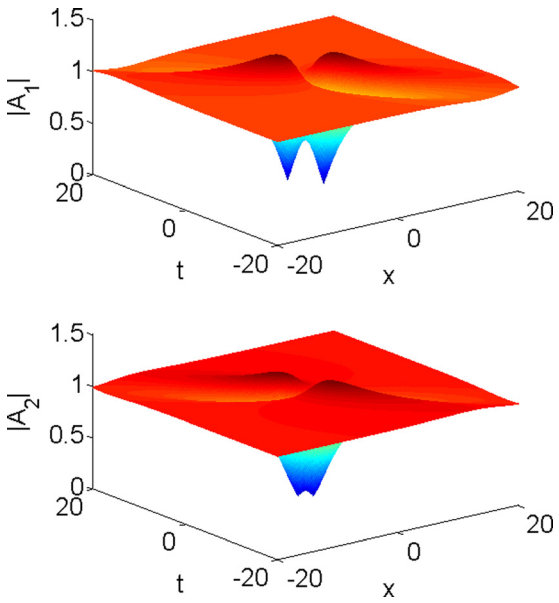

FIG. 2. Rogue waves as given in Eqs. (12) and (13) with $\alpha = 2$, $\beta = 1$, $\lambda = 2$, $\sigma = -1$, $\rho = 1$, and $\Omega_0 = -0.840 \pm 0.410i$. The parameter σ is negative, and hence each waveguide alone will not permit the existence of a rogue wave. The rogue wave results from modulation instability induced due to coupling.

possesses one maximum with an amplification ratio of three,[26] while the coupled case studied in this paper displays elevations, depressions, and four-petal configurations.[11,31]

A. Coupling induced existence regimes for rogue waves

It will be instructive to consider first the degenerate case $\alpha = \beta$, which will imply $A_1 = A_2$. The dispersion relation (11) becomes

$$(\alpha\Omega_0 + \lambda/\alpha)^2[(\alpha\Omega_0 + \lambda/\alpha)^2 + 4\sigma\rho^2{\Omega_0}^2] = 0.$$

This will yield complex roots for real α and λ only if the discriminant of the second quadratic expression is negative, i.e., $\sigma > 0$. Even for $\alpha \neq \beta$ ($A_1 \neq A_2$), complex roots (and hence rogue waves) will continue to exist for $\sigma > 0$. This can indeed be verified numerically (Table I) with $p = 1$.

For the regime $\sigma < 0$, rogue waves would not exist for the single component case, but *coupling will nevertheless give rise to these waves*. This can again be checked numerically (Table II) with $p = 1$.

B. Wave profiles

Wave profiles can typically be classified geometrically as one of the following shapes:

(a) one elevation accompanied by two depressions (Figure 1, lower panel) or one depression flanked by two elevations;
(b) a four-petal configuration which resembles the shape of a flower (Figure 1, upper panel).

New rogue waves produced by coupling for the case $\sigma < 0$ are illustrated in Figure 2.

C. Modifications of the wave profiles and a "black" rogue wave

The wave profiles of the component wave packets A_n, $n = 1, 2$, can display an intriguing sequence of changes on modifying the carrier wave number α. A typical example is illustrated in Figure 3, where A_1, A_2 are displayed in the left,

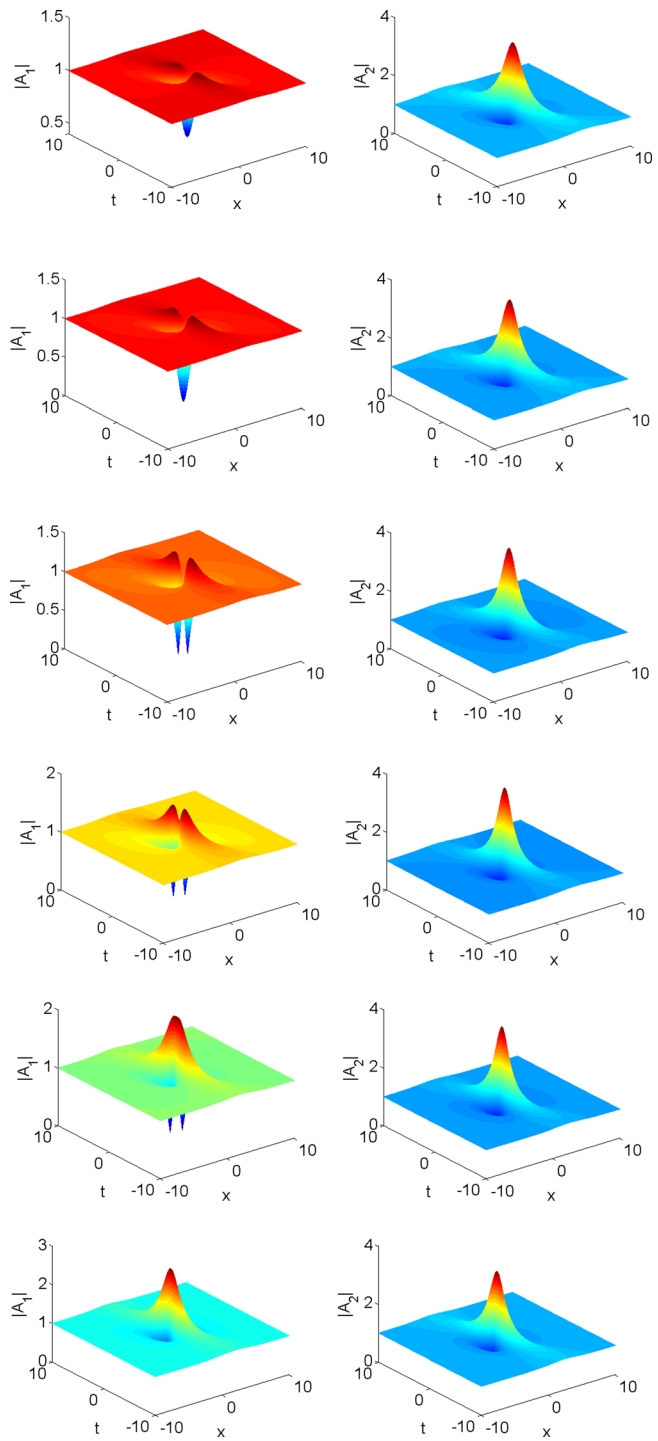

FIG. 3. Stages of transition from depression, four-petal to elevation rogue waves, $\beta = \lambda = \sigma = \rho = 1$, with values of α and Ω_0 given for each individual figures. The values of parameters from top to bottom are as follows. (a): $\alpha = 0.408$, $\Omega_0 = -0.309 \pm 0.490i$; (b): $\alpha = 0.508$, $\Omega_0 = -0.289 \pm 0.494i$; (c): $\alpha = 0.608$, $\Omega_0 = -0.263 \pm 0.491i$; (d): $\alpha = 0.708$, $\Omega_0 = -0.237 \pm 0.476i$; (e): $\alpha = 0.808$, $\Omega_0 = -0.218 \pm 0.453i$; and (f): $\alpha = 0.908$, $\Omega_0 = -0.206 \pm 0.426i$.

TABLE III. Distinct pairs of complex conjugate roots for the dispersion relation.

α	β	λ	σ	Ω_0	M_2
2	1	2	1	$-0.946 \pm 0.845i$	1.067
2	1	2	1	$-0.340 \pm 0.250i$	0.484

right column, respectively. Starting from a parameter regime where A_1, A_2 exhibit a "depression" and an "elevation" rogue wave (Figure 3(a)), changing α would deepen the depression until the "intensity" $|A_1|^2$ reaches zero, i.e., a "black" rogue wave (Figure 3(b)).

On further changing the wave number α, the minimum at $x=0$, $t=0$ is converted to a saddle point. Physically, this minimum is split into two smaller minima (Figure 3(c)). In the next stage, the two maxima now approach each other and merge into a single maximum (Figures 3(d) and 3(e)). Finally, a scenario with two elevation rogue waves is attained (Figure 3(f)).

IV. FURTHER NONLINEAR DYNAMICS

A. Multiple wave configurations

Distinct (or multiple) configurations of rogue wave profiles for the same input parameters are possible when there are two distinct (or multiple) pairs of complex roots for the dispersion relation. An illustrative example is given in Table III with $p=1$.

The first possible configuration is illustrated in Figure 1 (a four-petal for $|A_1|$ and an elevation for $|A_2|$), but the second complex root of the dispersion relation gives $\Omega_0 = -0.340 \pm 0.250i$, yielding a completely different wave profile (elevation, depression for $|A_1|$, $|A_2|$, Figure 4).

B. Simplification of the dispersion relation

Although the dispersion relation defined by a polynomial of the fourth order can be solved analytically in principle, the resulting expressions are usually complicated. Consequently, we shall instead examine a special case where the dispersion relation reduces to a cubic expression. This simplification is achieved for amplitude ρ and parameter σ satisfying the condition,

$$\sigma\rho^2 = -\alpha^2\beta^2/[2(\alpha^2+\beta^2)].$$

It proves to be convenient to define

$$z = \beta^2\Omega_0/\lambda, \sigma_0 = \sigma\rho^2/\beta^2, \quad \gamma = \alpha/\beta.$$

The dispersion relation then simplifies to

$$2\gamma^2(\gamma^4+1)z^3 + [\gamma^2(\gamma^2+2)^2+1]z^2 + 2(\gamma^2+1)^2 z + 1 + \gamma^2 = 0.$$

Roots of a cubic equation are dictated by a discriminant which reduces in this case to

$$\Delta = 4\gamma^2(\gamma^4-1)^2(\gamma^8-7\gamma^6+11\gamma^4-7\gamma^2+1).$$

The necessary and sufficient condition for complex conjugate wave numbers to occur is $\Delta<0$, i.e., $\gamma^2 \neq 1$ falling within the interval

$$\left(\frac{(-w_0+\sqrt{13}+7)}{4}, \frac{(w_0+\sqrt{13}+7)}{4}\right),$$
$$w_0 = 2\left[(23+7\sqrt{13})/2\right]^{1/2}$$

or γ^2 belonging to the range (0.196, 5.107). Rogue waves will always exist then as we can prove that M_2 is always positive under such conditions. For $z = a_1 + ib_1$ with a_1, b_1 real, we have

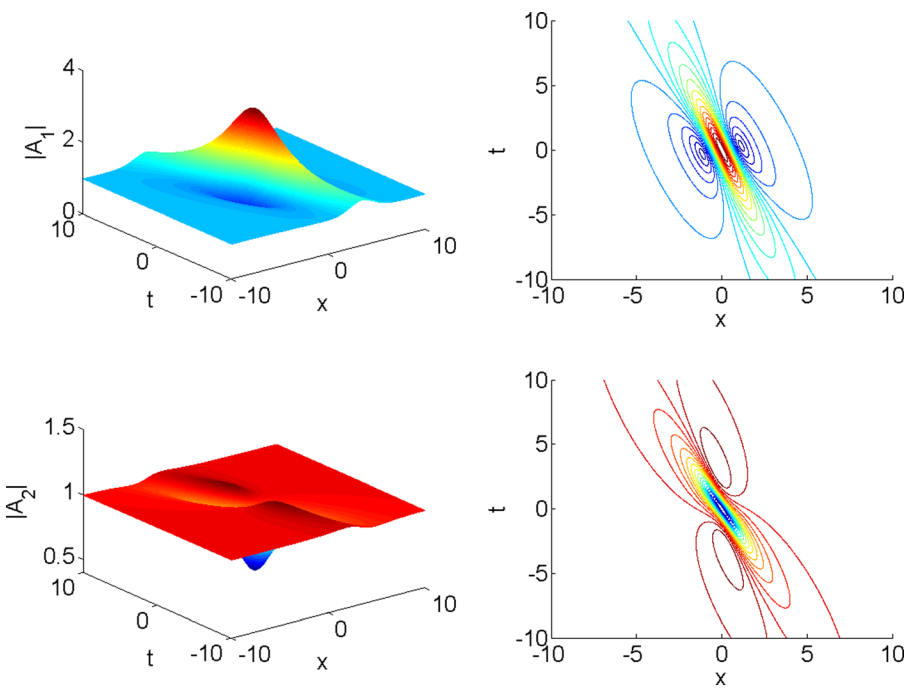

FIG. 4. Distinct rogue wave configurations corresponding to double (or multiple) eigenvalues of Eqs. (12) and (13): Same parameter values as those of Figure 1, i.e., $\alpha=2$, $\beta=1$, $\lambda=2$, $\sigma=1$, $\rho=1$, but with a different $\Omega_0 = -0.340 \pm 0.250i$. Hence, the wave profiles are different ($|A_1|$ in the top panel, $|A_2|$ in the bottom panel).

$$M_2 = -\frac{a_1(a_1^2 + b_1^2)}{\beta^2 b_1^2},$$

$$a_1 = -\frac{1}{12(\gamma^6+\gamma^2)}\left[2(\gamma^6+4\gamma^4+4\gamma^2+1) + \frac{(\gamma^6-2\gamma^4-2\gamma^2+1)^2}{\sqrt[3]{R(\gamma)}} + \sqrt[3]{R(\gamma)}\right],$$

$$R(\gamma) = -\gamma^{18} + 6\gamma^{16} - 6\gamma^{14} + 35\gamma^{12} - 30\gamma^{10} - 30\gamma^8 + 35\gamma^6 - 6\gamma^4 + 6\gamma^2 + 6\sqrt{3}\sqrt{-\gamma^6(\gamma^8-1)^2(\gamma^8-7\gamma^6+11\gamma^4-7\gamma^2+1)} - 1.$$

One may check readily that, for $\gamma^2 \neq 1$ falling within the above interval, $R(\gamma)$ is positive, which implies that a_1 is negative. Consequently, M_2 is always positive and nonsingular rogue waves exist.

V. MODULATION INSTABILITIES

A plane or continuous wave solution with distinct background amplitudes (ρ and χ) of the coupled system (6) is given by

$$A_1 = \rho \exp[i(\alpha x - \lambda t/\alpha)], \quad A_2 = \chi \exp[i(\beta x - \lambda t/\beta)], B = 0. \tag{14}$$

Imposing small perturbations and searching for modes proportional to $\exp[i(rx - st)]$ will give the frequency s in terms of the wavenumber r. We focus on the long wave regime ($r, s \to 0$), with $s/r = c$ being of order unity, and we find that

$$(\alpha c + \lambda/\alpha)^2(\beta c + \lambda/\beta)^2 + 2\sigma c^2[\rho^2(\alpha c + \lambda/\alpha)^2 + \chi^2(\beta c + \lambda/\beta)^2] = 0. \tag{15}$$

However, in searching for modulation instability, the perturbation needs to be expressed in the original space and time variables, so that on using (4), $rx - st = KX - \zeta T$ where $K = r + s/c_2$, $\zeta = c_1 r + s$. Modulation instability arises when ζ is complex-valued for a real wavenumber K, and hence $c = s/r$ is also complex-valued. Equation (15) is a quartic equation for c, and if $\sigma > 0$, there are no real solutions for c and all four solutions for c are complex, indicating the presence of modulation instability (or existence of rogue waves). For $\sigma < 0$ and $\alpha = \beta$ (which imply A_2 proportion to A_1) in the plane wave solution Eq. (14), all solutions for c are real and there is no modulation instability. However, for $\sigma < 0$ and $\alpha \neq \beta$, then two complex roots for c can be found, and modulation instability arises, consistent with the existence of rogue waves in this case.

Furthermore, for the special case of equal background amplitude ($\rho = \chi$), Eq. (15) for the onset of modulation instability degenerates to

$$(\alpha c + \lambda/\alpha)^2(\beta c + \lambda/\beta)^2 + 2\sigma\rho^2 c^2[(\alpha c + \lambda/\alpha)^2 + (\beta c + \lambda/\beta)^2] = 0,$$

which remarkably is exactly Eq. (11), i.e., the existence condition of rogue waves. Physically, this confirms again the intimate relation between the onset of modulation instability and the existence criterion for rogue waves. Regarding the

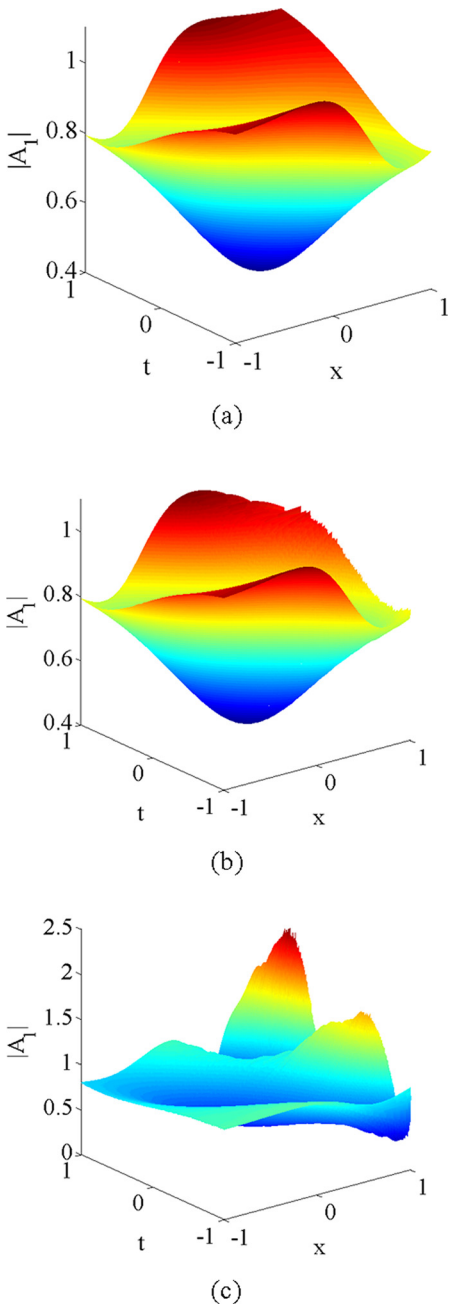

FIG. 5. (a) Numerical marching forward in time for A_1 with the exact solution Eq. (13) as the boundary and initial conditions, $\alpha = 0.408$, $\beta = 1$, $\lambda = 1$, $\sigma = 1$, $\rho = 1$, $a = -0.309$, and $b = 0.490$, maximum normalized modulation instability growth rate Eq. (15) (imaginary part of c) $= 2.020$. (b) Evolution of the depression rogue wave with a noise of 0.1% at the boundary. (c): Evolution of the depression rogue wave with a noise of 1% at the boundary. The rogue wave is severely distorted.

actual growth rates, coupling generally produces a higher amplification ratio than that of the single component system.

Verification by numerical studies

This intrinsic presence of modulation instability might also lead to the growth of background noise, as wavenumbers corresponding to a whole unstable band might amplify. To examine this idea, we simulate the evolution of a rogue wave directly. Finite difference schemes were developed for Eq. (6). Our focus will be placed on the evolution of the rogue waves, and a computational domain in the (x, t)-plane containing the rogue wave is chosen. Random noise is added to the boundary condition and the evolution of the amplitude is marched forward in space/time coordinates numerically. This evolution will be compared with that of a control simulation without background noise.

(a) The evolution of the exact solution for one component say, A_1 is illustrated in Figure 5(a), where a depression rogue wave is observed.

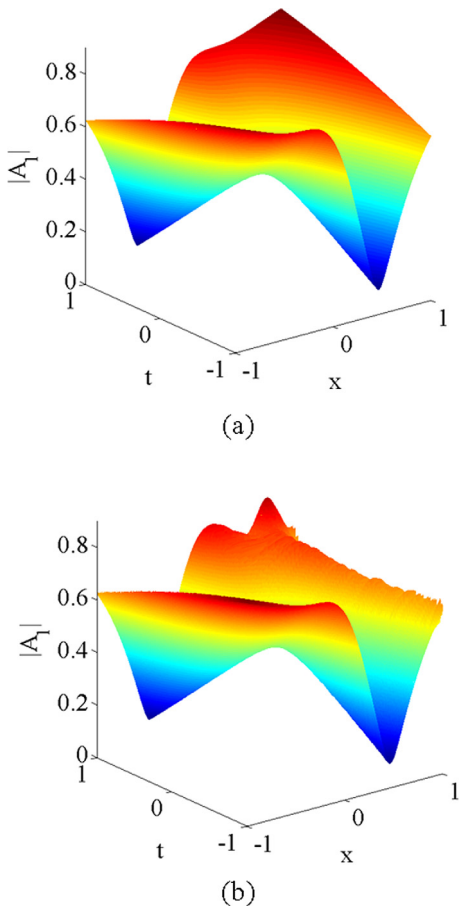

FIG. 6. (a) Numerical marching forward in time for A_1 with the exact solution Eq. (13) as the boundary and initial conditions, but with a different set of parameters from Figure 5(a), and hence a different modulation instability growth rate: $\alpha = 0.9$, $\beta = 1.45$, $\lambda = 0.5$, $\sigma = 1$, $\rho = 1$, $a = -0.111$, and $b = 0.134$. (b) Evolution of the rogue wave with a noise of 1% at the boundary. This smaller growth rate of 0.198 compared with 2.020 of Figure 5(a) implies that the competition from background noise is less severe, and the rogue wave is more prominent, but the growth of the perturbation noise can be observed in the background.

- If a very weak (extremely small amplitude) noise of 0.1% is imposed, the rogue wave is basically unaffected (Figure 5(b)).
- If a moderate noise of 1% is imposed, the shape of the rogue wave is severely distorted (Figure 5(c)).

(b) We also consider a different set of parameters where the growth rate from modulation instability is less substantial (Figure 6(a) for the exact solution). Under perturbations with a 1% noise, the bulk shape of the rogue wave can still be observed, but the growth of the perturbation noise can be detected in the background (Figure 6(b)). We expect the degree of distortion of the rogue wave to increase with the magnitude of the intrinsic modulation instability.

VI. DISCUSSION AND CONCLUSIONS

A nonlinear evolution system modeling geophysical flows describing baroclinic instability processes is studied. By incorporating two (or in general multiple) packets of short waves, new regimes of modulation instabilities and rogue waves will arise. From a theoretical perspective, the onset of modulation instabilities correlates in this system precisely with the existence criterion for rogue waves. Indeed the present dynamical system might serve as another analytically tractable model for coupled waveguides in addition to the existing few, intensively studied ones, e.g., the coupled NLS (Manakov) equations. More precisely, features illustrative of the nonlinear dynamics are

- The transitions among elevation, depression, and four-petal configurations of rogue waves are elucidated analytically. Geometrically these transitions are similar to those exhibited by the coupled NLS (Manakov) equations.[33]
- Two distinct pairs of complex conjugate roots are possible for the dispersion relation in the long wave limits, resulting in different rogue wave configurations for the same input parameters physically.

In terms of future work, further theoretical works can be pursued along these lines:

- Higher order rogue waves can be calculated using a multiple breather asymptotic expansion as the starting point, followed by taking a long wave limit.
- Further tests on the structural stability of the rogue waves need to be investigated by numerical simulations.[34,35]
- Finally, the physical implications and verifications of these theoretical predictions should be examined. The amplitude and time scale of these rogue waves in terms of actual numerical values should be compared with field data.

Further fruitful results await future efforts of researchers.

ACKNOWLEDGMENTS

Partial financial support has been provided by the Research Grants Council through Contract Nos. HKU 711713E, HKU704611P, and HKU17200815. Dr. J. H. Li of Nanjing University of Information Science and Technology assisted in the numerical simulations.

[1]Y. S. Kivshar and S. Flach, "Introduction: Nonlinear localized modes," Chaos **13**, 586 (2003).
[2]K. Dysthe, H. E. Krogstad, and P. Müller, "Oceanic rogue waves," Annu. Rev. Fluid Mech. **40**, 287 (2008).
[3]C. Kharif and E. Pelinovsky, "Physical mechanisms of the rogue wave phenomenon," Eur. J. Mech., B: Fluids **22**, 603 (2003).
[4]M. Onorato, A. R. Osborne, and M. Serio, "Modulation instability in crossing sea states: A possible mechanism for the formation of freak waves," Phys. Rev. Lett. **96**, 014503 (2006).
[5]D. Clamond, M. Francius, J. Grue, and C. Kharif, "Long time interaction of envelope solitons and freak wave formations," Eur. J. Mech., B: Fluids **25**, 536 (2006).
[6]M. Onorato, S. Residori, U. Bortolozzo, A. Montin, and F. T. Arecchi, "Rogue waves and their generating mechanisms in different physical contexts," Phys. Rep. **528**, 47 (2013).
[7]R. Grimshaw, E. Pelinovsky, T. Talipova, and A. Sergeeva, "Rogue internal waves in the ocean: Long wave model," Eur. Phys. J.: Spec. Top. **185**, 195 (2010).
[8]D. R. Solli, C. Ropers, P. Koonath, and B. Jalali, "Optical rogue waves," Nature **450**, 1054 (2007).
[9]A. D. D. Craik, *Wave Interactions and Fluid Flows* (Cambridge University Press, 1985).
[10]Y. S. Kivshar and G. P. Agrawal, *Optical Solitons: From Fibers to Photonic Crystals* (Academic Press, 2003).
[11]J. He, L. Guo, Y. Zhang, and A. Chabchoub, "Theoretical and experimental evidence of non-symmetric doubly localized rogue waves," Proc. R. Soc. A **470**, 20140318 (2014).
[12]M. J. Ablowitz and T. P. Horikis, "Interacting nonlinear wave envelopes and rogue wave formation in deep water," Phys. Fluids **27**, 012107 (2015).
[13]V. I. Shrira and V. V. Geogjaev, "What makes the Peregrine soliton so special as a prototype of freak waves?" J. Eng. Math. **67**, 11 (2010).
[14]R. Grimshaw, A. Slunyaev, and E. Pelinovsky, "Generation of solitons and breathers in the extended Korteweg-de Vries equation with positive cubic nonlinearity," Chaos **20**, 013102 (2010).
[15]V. Zakharov and A. Gelash, "Freak waves as a result of modulation instability," Proc. IUTAM **9**, 165 (2013).
[16]H. N. Chan, K. W. Chow, D. J. Kedziora, R. H. J. Grimshaw, and E. Ding, "Rogue wave modes for a derivative nonlinear Schrödinger model," Phys. Rev. E **89**, 032914 (2014).
[17]A. J. Whitfield and E. R. Johnson, "Modulational instability of co-propagating internal wavetrains under rotation," Chaos **25**, 023109 (2015).
[18]B. A. Malomed, "Solitary pulses in linearly coupled Ginzburg-Landau equations," Chaos **17**, 037117 (2007).
[19]F. Baronio, M. Conforti, A. Degasperis, S. Lombardo, M. Onorato, and S. Wabnitz, "Vector rogue waves and baseband modulation instability in the defocusing regime," Phys. Rev. Lett. **113**, 034101 (2014).
[20]L. Shemer and L. Alperovich, "Peregrine breather revisited," Phys. Fluids **25**, 051701 (2013).
[21]A. Chabchoub, N. Hoffmann, M. Onorato, and N. Akhmediev, "Super rogue waves: Observation of a higher-order breather in water waves," Phys. Rev. X **2**, 011015 (2012).
[22]B. Tan and J. P. Boyd, "Envelope solitary waves and periodic waves in the AB equations," Stud. Appl. Math. **109**, 67 (2002).
[23]I. M. Moroz and J. Brindley, "Evolution of baroclinic wave packets in a flow with continuous shear and stratification," Proc. R. Soc. London **377**, 379 (1981).
[24]J. D. Gibbon, I. N. James, and I. M. Moroz, "An example of soliton behavior in a rotating baroclinic fluid," Proc. R. Soc. London **367**, 219 (1979).
[25]R. Guo, H. Q. Hao, and L. L. Zhang, "Dynamic behaviors of the breather solutions for the *AB* system in fluid mechanics," Nonlinear Dyn. **74**, 701 (2013).
[26]X. Wang, Y. Li, F. Huang, and Y. Chen, "Rogue wave solutions of *AB* system," Commun. Nonlinear Sci. Numer. Simul. **20**, 434 (2015).
[27]Y. Matsuno, *The Bilinear Transformation Method* (Academic Press, 1984).
[28]R. Hirota, *The Direct Method in Soliton Theory* (Cambridge University Press, 2004).
[29]K. W. Chow, H. N. Chan, D. J. Kedziora, and R. H. J. Grimshaw, "Rogue wave modes for the long wave-short wave resonance model," J. Phys. Soc. Jpn. **82**, 074001 (2013).
[30]B. G. Zhai, W. G. Zhang, X. L. Wang, and H. Q. Zhang, "Multi-rogue waves and rational solutions of the coupled nonlinear Schrödinger equations," Nonlinear Anal.: Real World Appl. **14**, 14 (2013).
[31]N. V. Priya, M. Senthilvelan, and M. Lakshmanan, "Akhmediev breathers, Ma solitons, and general breathers from rogue waves: A case study in the Manakov system," Phys. Rev. E **88**, 022918 (2013).
[32]Yu. V. Bludov, V. V. Konotop, and N. Akhmediev, "Vector rogue waves in binary mixtures of Bose-Einstein condensates," Eur. Phys. J.: Spec. Top. **185**, 169 (2010).
[33]L. C. Zhao and J. Liu, "Rogue-wave solutions of a three-component coupled nonlinear Schrödinger equation," Phys. Rev. E **87**, 013201 (2013).
[34]N. Akhmediev, A. Ankiewicz, and J. M. Soto-Crespo, "Rogue waves and rational solutions of the nonlinear Schrödinger equation," Phys. Rev. E **80**, 026601 (2009).
[35]A. Ankiewicz, J. M. Soto-Crespo, and N. Akhmediev, "Rogue waves and rational solutions of the Hirota equation," Phys. Rev. E **81**, 046602 (2010).